NANO LETTERS

pubs.acs.org/NanoLett

Suppression of Auger Processes in Confined Structures

George E. Cragg,* and Alexander L. Efros*

Naval Research Laboratory, Washington, D.C. 20375

ABSTRACT We explore how the size and shape of the microscopic confinement potential affects the nonradiative Auger decay rate of confined carriers. Calculations conducted in the two-band, effective mass Kane model unambiguously show that smoothing out the confinement potential could reduce the rate by more than 3 orders of magnitude relative to the rate in structures with abruptly terminating boundaries. As the confinement potential width is increased, the calculated rate decreases overall, exhibiting very deep minima at regular widths. Such minima suggest that nanocrystals of "magic sizes" can exist for which nonradiative Auger processes are strongly suppressed.

KEYWORDS Auger processes, quantum dot, quantum well, quantum wire, nanocrystal blinking, laser threshold

In the early sixties, the one-dimensional carrier confinement achieved in semiconductor quantum wells and superlattices brought about a revolution in solid-state device technology. To fulfill the requirements of miniaturization, low power consumption and fast operational speed, further efforts of carrier confinement in two and in three dimensions were realized with the advent of quantum wires and quantum dots. However, the application of nanostructures to real-world devices has been strongly curtailed by the enhancement of dissipative Auger processes that undergird all aspects of carrier relaxation and recombination. In particular, Auger processes have been attributed to the decrease of the photoluminescence (PL) quantum efficiency in light emitting diodes,[1] an increase in the stimulated emission threshold in lasers,[2] and the PL degradation[3,4] and PL blinking[5] in nanocrystal (NC) quantum dots.

These detrimental effects were initially explained through other mechanisms since bulk wide-gap semiconductors have negligible Auger rates due to a temperature threshold proportional to their energy gap.[6] Eventually, it was realized that the temperature threshold was not present because, unlike the requirement in the bulk case, Auger recombination in confined structures does not require a carrier with kinetic energy comparable to the energy gap.[3,7,8] This explained why Auger processes were very efficient in confined structures, even those fabricated from wide-gap semiconductors.

Most impressively, Auger processes are visually manifest in the random intermittency observed in studies of the PL intensity emitted from a single NC. Even under constant illumination, all colloidal NCs grown today exhibit this emission intermittency which has consequently been dubbed "photoluminescence blinking." First observed twelve years ago, the intermittency of the photoluminescence intensity came as a complete surprise in a study of single CdSe NCs under steady-state excitation conditions.[5] Since then, many other groups have observed this effect at various temperatures in many other types of NCs and nanowires.[9]

Today, consensus is that blinking occurs because NCs can undergo a random process of charging and discharging while under constant illumination.[10] Optical excitation creates an electron−hole pair which then recombines giving rise to PL in a neutral NC. However, if the NC is charged, the extra carrier triggers a process known as nonradiative Auger recombination during which the exciton energy is acquired by the extra charging electron or hole (see Figure 1). Because the rate of Auger recombination is orders of magnitude faster than the rate of radiative recombination,[3] photoluminescence is completely suppressed or "quenched" in charged NCs.

In this letter, we calculate the efficiency of Auger processes in low-dimensional heterostructures that confine the free motion of carriers. Specifically, we demonstrate that the enhanced efficiency of Auger processes is due to the abruptness of the heterointerfaces or bounding surfaces, thereby suggesting a natural way of suppressing Auger efficiency through the creation of structures having a soft confining potential. This conjecture is confirmed by calculations that show several orders of magnitude in suppression of the nonradiative Auger decay rate for confinement potentials with smooth profiles. Lastly, Auger processes become quenched at certain "magic sizes" of the confinement potential width due to destructive interference between the initial and the final states.

The rate of nonradiative Auger recombination can be calculated using Fermi's Golden Rule[11]

$$\frac{1}{\tau_A} = \frac{2\pi}{\hbar}\int |M_{if}|^2 \delta(E_i - E_f) d\mathcal{R}_f \qquad (1)$$

where M_{if} is the electronic transition matrix element of the interparticle Coulomb interaction, $E_{i(f)}$ is the initial (final) energy of the system (see Figure 1b,c, for example), and $\mathcal{R}_f$

* To whom correspondence should be addressed. E-mail: cragg@alum.mit.edu (G.E.C.); efros@dave.nrl.navy.mil (A.L.E.).

Received for review: 10/27/2009
Published on Web: 12/17/2009

DOI: 10.1021/nl903592h | *Nano Lett.* **2010,** *10,* 313-317

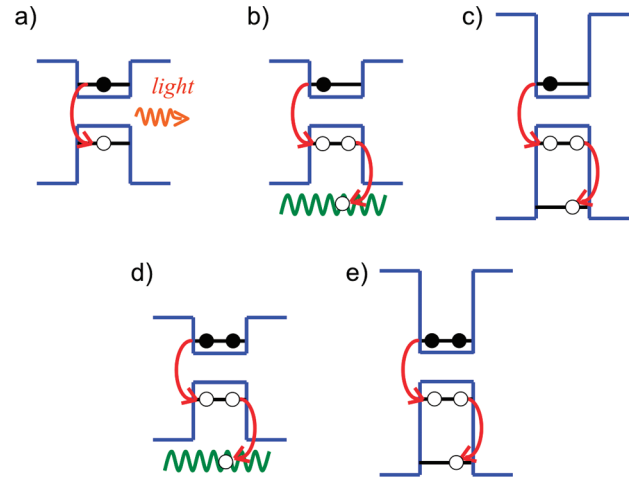

FIGURE 1. A schematic diagram showing various recombination processes of photoexcited electron−hole pairs. Panel (a) depicts a neutral structure in which a photoexcited electron−hole pair recombines then radiatively emits light. If the structure acquires a positive charge, for example, then the excitation energy of the electron−hole pair is transferred to the extra hole. In this nonradiative Auger recombination process, the remnant hole will either be ejected into the continuum (shown as a sinusoidal wave) (b) or it will remain bound inside the nanostructure for sufficiently deep confinement (c). Even in the case of multiple excitons, Auger processes lead either to carrier excitation in the continuum (d) or to a bound level (e). Similar figures can be displayed for the case where the extra charge is an electron instead of a hole.

is the complete set of variables quantifying the final state of the system. Because highly excited final states are short-lived relative to the Auger transition time, eq 1 provides a valid description of the Auger rate[12] for a final hole state that is either bound or that resides in the continuum.

When calculating the Auger rate, a major problem is encountered in obtaining an accurate estimation of the transition matrix element, M_{if}, in eq 1. After the Auger process, the extra carrier acquires a large momentum, $\hbar k_f$, as a result of the transfer of the photoexcitation energy (see Figure 1). Consequently, the corresponding wave function becomes rapidly oscillating,[3] resulting in a matrix element that is much smaller than the average Coulomb interaction energy, $e^2/\kappa a$, where κ is the dielectric constant and a is the typical confinement size. Integration of the smooth ground state with the rapidly oscillating final state causes the relative diminution in M_{if}.

From the Fourier expansion of the ground state, the leading contribution to M_{if} is given by the spatial frequency component, k_F, which matches the large momentum of electrons or holes in the excited final state, $k_F \approx k_f$. In heterostructures, the large k_F is usually generated by abrupt interfaces or surfaces. For example, the particle-in-box ground state wave function, $\psi(x) = \sin[\pi(1 - x/a)/2]/\sqrt{a}$, has a Fourier transform proportional to $1/(k_F a)^2$, where a is the half-width of the box. In contrast, the ground state wave function for a parabolic potential, $\exp(-x^2/2a^2)/(\sqrt{\pi}a)^{1/2}$, has a Fourier transform proportional to $\exp(-k_F^2 a^2/2)$. At large $k_F = k_f \gg 1/a$, the Fourier component corresponding to the abrupt box potential is exponentially larger than that associated with a smooth, parabolic profile. Apparently, increasing the abruptness of a confinement potential concomitantly increases the matrix element M_{if}, thus accelerating the rate of Auger processes. This qualitative analysis indicates that Auger processes would be significantly suppressed in low-dimensional structures with a soft confinement potential.

To test this idea quantitatively, we calculate the Auger recombination rate for the specific case of a two-hole plus one electron trion described by a two-band Kane model where both electrons and holes are confined by an identical one-dimensional potential

$$U_e(x) = U_h(x) = U_0 \frac{x^\nu}{x^\nu + a^\nu} \tag{2}$$

In this expression, $2a$ is the effective width of the confinement potential, U_0 is the potential height, and ν controls the smoothness. That is, the confining boundary becomes sharper with increasing ν, approaching a discontinuous step in the limit $\nu \to \infty$. For this model, the other extreme is the smoothest possible potential at $\nu = 2$, which has a parabolic shape at the conduction and valence band edges. Such smooth potentials could be created, for instance, by gradually changing the average alloy composition in a quantum well.[14] We consider only the case of strong confinement, where the Bohr radius of the bulk exciton, a_B, is much larger than a. Since carrier confinement energies must then be larger than the Coulombic interaction energies, a first approximation treats the trion energy as a spectrum of independent quantized particles while Coulomb correlations can be calculated perturbatively.[13]

Confined, noninteracting electrons and holes in the two-band Kane model[15] are described by the Hamiltonian

$$\hat{H} = \begin{pmatrix} (\alpha_e/2m_0)\hat{p}^2 + E_g/2 + U_e(x) & K\hat{p} \\ K\hat{p} & -(\alpha_h/2m_0)\hat{p}^2 - E_g/2 - U_h(x) \end{pmatrix} \tag{3}$$

where $\hat{p} = -i\hbar\partial/\partial x$ is the momentum operator, E_g is the energy gap, K is the Kane matrix element that describes coupling between conduction and valence bands, m_0 is the mass of the free electron, and $\alpha_{e(h)}$ is the contribution of the remote bands to the effective masses of electrons (holes). With this notation, the effective mass of an electron at the bottom of the conduction band, m_e, and the effective mass of a hole at the top of the valence band, m_h, are written as $1/m_e = \alpha_e/m_0 + 2K^2/E_g$ and $1/m_h = \alpha_h/m_0 + 2K^2/E_g$, respectively.

To find the electron and hole spectra described by eq 3, we calculate the matrix form of this Hamiltonian in an orthogonal basis chosen for computational convenience.[16] In selecting such a basis it is natural to consider independent electrons and holes as described by the respective Hamiltonian operators $\hat{H}_e = (\alpha_e/2m_0)\hat{p}^2 + E_g/2$ and $\hat{H}_h = -(\alpha_h/2m_0)\hat{p}^2 - E_g/2$. Additionally, the space can be discretized by demanding that the basis functions vanish at a boundary, $x = \pm L$, that is much larger

DOI: 10.1021/nl903592h | *Nano Lett.* **2010,** *10,* 313-317

than the size of the confinement potential, a.[17] Because the basis wave functions are simple sines and cosines, the matrix form of the Hamiltonian (eq 3), H_{ij}, may be efficiently calculated. Finally, standard numerical diagonalization routines are employed to obtain the energy spectra along with the corresponding eigenvectors for the matrix H_{ij}.

Positively charged trions undergo Auger recombination when the electron−hole pair annihilates then transfers its entire energy to the excess hole. Depending on whether the height of the localizing potential, U_0, is smaller than or larger than the annihilation energy, the remnant hole will either reside in a continuum or in a discrete state (see Figures 1b,c). Regardless, the matrix element of Auger transitions, M_{if}, should be considered within the electron−electron or the hole−hole representation. Positively charged trions correspond to the latter, where the Auger process occurs due to the Coulomb interaction between two holes of opposite spins that occupy the ground state hole levels of the confinement potential. As a result of the Coulomb interaction, one of these holes is transferred to the conduction band, replacing an electron at the lowest electron level (this is the electron−hole annihilation), while the second hole jumps to some highly excited state in the valence band.

In the strongly confined regime, both the initial state wave function and the final state wave function can be written as an antisymmetrized product of the single-hole wave functions. Denoting ψ_h^0 as the wave function of the single-hole ground state,[16] and λ and β as the spinors of the states having spin projections of $\pm 1/2$, the initial, two-hole wave function can be written as

$$\Psi^i(x_1, x_2) = \frac{1}{\sqrt{2}}\psi_h^0(x_1)\psi_h^0(x_2)[\lambda(1)\beta(2) - \lambda(2)\beta(1)] \quad (4)$$

Similarly, the two-hole wave function of the final state is

$$\Psi^f(x_1, x_2) = \frac{1}{2}[\psi_e^0(x_1)^*\phi_f(x_2) + \psi_e^0(x_2)^*\phi_f(x_1)][\lambda(1)\beta(2) - \lambda(2)\beta(1)] \quad (5)$$

where ψ_e^{0*} is a hole wave function, regarded as the complex-conjugate of the electron ground state, while ϕ_f is the wave function of the extra, excited hole. Should ϕ_f lie in the continuum, box-normalization is imposed to preserve normalization to the Kronecker delta function, $\langle\phi_{k_f}|\phi_{k'_f}\rangle = \delta_{k_f k'_f}$.

Using these wave functions, we calculate the matrix element, M_{if}, responsible for Auger recombination in the confined, one-dimensional model

$$M_{if} = \langle\Psi^i|V(x_1 - x_2)|\Psi^f\rangle$$

$$= \sqrt{2}\int dx_1\, dx_2\, \psi_h^0(x_1)^*\psi_h^0(x_2)^*V(x_1 - x_2)\psi_e^0(x_1)^*\phi_f(x_2) \quad (6)$$

Coulomb repulsion between the two holes is described by $V(x_1 - x_2) = (e^2/\kappa)/(|x_1 - x_2| + \delta)$ with the parameter $\delta = 10^{-2}$nm introduced to keep the interaction well-defined at small distances.[18] First consider the case where Auger recombination leads to ejection of the hole from the confinement potential (see Figure 1b). Since the final hole state is in the continuum, energy conservation simplifies the Auger rate, $1/\tau_A$, of eq 1 to a product involving the density of final states, $\rho(E_f)$

$$\frac{1}{\tau_A} = \frac{2\pi}{\hbar}|M_{if}|^2\rho(E_f) \quad (7)$$

Equation 7 quantitatively shows that in the limit $k_f a \gg 1$, the Auger rate is proportional to the square of the Fourier transform of the ground state wave function, $|\tilde{\psi}_h^0(k_f)|^2 = |\int_{-\infty}^{\infty} dx\, \psi_h^0(x)\exp(ik_f x)|^2$. From the Fourier integral representation of the Coulomb potential, $1/(|x_1 - x_2| + \delta) = (1/2\pi)\int_{-\infty}^{\infty} dq \exp[-iq(x_1 - x_2)]\tilde{V}(q)$, we have[16]

$$M_{if} \simeq \frac{e^2}{\kappa}\frac{\sqrt{2}}{2\pi}\tilde{\psi}_h^0(k_f)^*\int_{-1/a}^{1/a} dq\, \tilde{V}'(q) \quad (8)$$

where $\tilde{V}'(q) = \tilde{V}(q)\int_{-\infty}^{\infty} dx \exp(-iqx)\psi_h^0(x)^*\psi_e^0(x)^*$, $\tilde{V}(q) = -Ei(-iq\delta)\exp(iq\delta) - Ei(iq\delta)\exp(-iq\delta)$, and Ei is the exponential integral.[18] As a result, $1/\tau_A \sim |\tilde{\psi}_h^0(k_f)|^2$.

Suppression of the Auger rate is accomplished by softening the confining potential, causing an attenuation of the high frequency components in the ground state hole wave function. Figure 2 shows how the Auger recombination rate of eq 7 varies

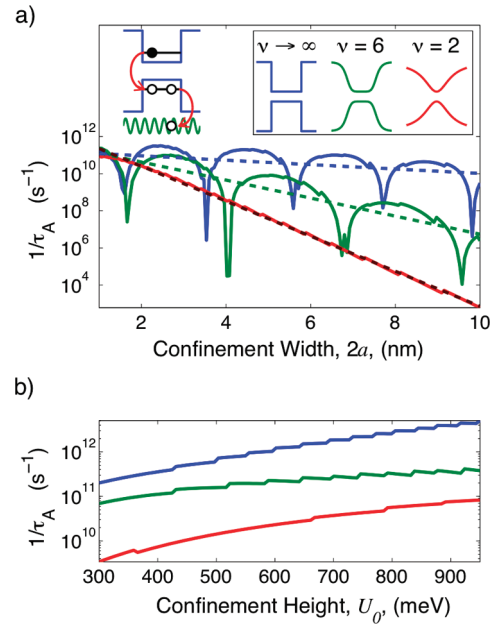

FIGURE 2. (a) Semilog plot of the Auger recombination rate as a function of the confinement potential width, 2a, for the case where the hole is ejected into the continuum (upper left). As shown in the inset, the three traces correspond to the confinement profiles given by eq 2 for $\nu \to \infty$ (blue), 6 (green), and 2 (red), each with a fixed height of $U_0 = 300$ meV. Accompanying dashed lines are best fits to the dependencies in the least-squares sense. (b) Semilog plot of the Auger recombination rate versus the confinement height calculated for the same confinement profiles, all having a fixed width of 2a = 3 nm. Here and throughout, we used an outer boundary of $L = 50$ nm.[17] The remaining quantities used in these calculations are typical for AlGaInAs/InP quantum wells, $\alpha_e = 25$, $\alpha_h = 1$, $E_g = 1$ eV, $U_0 = 300$ meV, $K = (21eV/2m_0)^{1/2}$, and $\kappa = 6$. This parameter set gives $a_B \approx 21.6$ nm, thus satisfying the strong confinement condition, $a < a_B$,[13] for all investigated widths of the confinement potential.

with both the width, $2a$, and the height, U_0, of the confinement potential for three shapes, $\nu \rightarrow \infty$, $\nu = 6$, and $\nu = 2$, given by eq 2. Depicted in the inset, the shape of the potential is gradually changed from a rectangular well at $\nu \rightarrow \infty$ to a very soft confinement at $\nu = 2$. In addition to the strong oscillatory behavior seen for $\nu \rightarrow \infty$ and $\nu = 6$, all traces exhibit a predominant decline with increasing width. Best-fit, dashed lines in Figure 2a show that smoothing the confining profile steepens the decline of the Auger rate. For example, at $2a = 5$ nm, these slopes are such that the smoothest profile at $\nu = 2$ has an Auger rate that is approximately 3 orders of magnitude lower than that for the abrupt step of $\nu \rightarrow \infty$. Also, Figure 2b shows a significant increase in the Auger rate caused by the additional abruptness associated with increasing confinement height, U_0. This numerical analysis confirms that softening the confinement potential prominently decreases the rate of nonradiative Auger recombination.

Furthermore, the orders-of-magnitude oscillations seen in Figure 2a arise out of an intrinsic symmetry of the problem. Similar oscillations have been found in the Auger recombination rate for a three-dimensional confinement potential analyzed using both the multiband effective mass approximation[3] and a first-principles calculation.[19] Because the Auger process does not change the initial symmetry of the multiparticle system, this symmetry must be maintained in the final state to obtain a nonvanishing matrix element. Therefore, the Auger recombination rate reaches a maximum when energy conservation allows the excited electron or hole to reach a quasiresonant level of the continuum with matching symmetry. For one-dimensional confinement, we call the matching symmetry state "even," whereas the corresponding three-dimensional case has a matching state with p-symmetry.[3] Conversely, the absence of such quasiresonant states leads to destructive quantum mechanical interference of the electron or hole wave functions[3] and consequently to the deep minima shown in the Auger recombination rate.

Analysis of the Auger recombination rate becomes more complicated if the confinement potential height is larger than the recombination energy acquired by the hole during the Auger process. Because of the resulting discreteness of the hole energy spectrum (see Figure 1c), energy conservation cannot always be satisfied. Additionally, transitions to some of these levels are forbidden by the selection rules dictated by the confinement potential symmetry. That is, the extra hole can only be excited to an even level of the one-dimensional confinement and only to a p-level of the three-dimensional, spherically symmetric confinement.[3] Hence, confinement potentials of certain sizes could have suppressed Auger recombination rates due to constraints imposed by these selection rules.

However, complete suppression of Auger processes does not occur, as the remnant hole can access highly excited levels that are strongly broadened by fast decay and dephasing. Defining the total dephasing rate of the final hole state by Γ_f, the Auger rate from eq 1 assumes the form

$$\frac{1}{\tau_A} = \frac{2\pi}{\hbar}|M_{if}|^2\frac{1}{\Gamma_f} \tag{9}$$

Similar to the previous case, $|M_{if}|^2$ controls the dependence of the Auger relaxation rate on both the width and the shape of the confinement potential. Figure 3 shows the dependence of $|M_{if}|^2$ on the width of the confinement, calculated for three different degrees of softness: $\nu = 2$, 4, and ∞. At each width, $|M_{if}|^2$ is calculated using the even excited state closest to that required by energy conservation. When a particular state ceases to be closest in energy, a discontinuous jump in the value of $|M_{if}|^2$ is obtained from the switch to another level that more closely satisfies energy conservation. Although softening the confining potential profile suppresses $|M_{if}|^2$, the reduction in the Auger rate is much less pronounced than it was when the extra carrier was ejected from the confinement potential.

To the best of our knowledge, there have been no systematic experimental studies addressing the effects of confinement shape on the rate of Auger processes in low-dimensional structures. Presently, however, Wang et al.[20] reported the observation of single NCs that do not show any blinking on time scales of hours. Surrounded by a ZnSe shell, these NCs have a $Cd_xZn_{1-x}Se$ core in which the alloying concentration, x, decreases with distance from the center. Gradation in this alloy structure suggests that there is a soft confining potential for both electrons and holes. Furthermore, the observed multipeak PL spectrum indicates that these NCs were charged.[20] Observation of PL from charged, nonblinking NCs can only be attributed to Auger recombination rate suppression, a conclusion strongly supported by the estimations conducted in ref 20 that give a nonradiative Auger recombination time of $\tau_A \sim 10$ ns, which is 2 or 3 orders of magnitude longer than that measured in standard core/shell NCs.[21]

Suppression of Auger rates was also observed in refs 22−24. Reference 22 reported a "gray state" of PL, likely connected with charged NCs, whose τ_A was only five times shorter than the radiative recombination time. Also, the

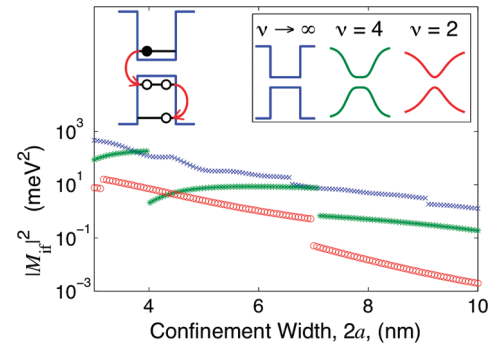

FIGURE 3. Semilog plot of the transition matrix element $|M_{if}|^2$ versus the width of the confinement potential, $2a$, for the case where the excited hole remains confined, depicted in the upper left. Each plot corresponds to a confining potential profile described by eq 2 for $\nu \rightarrow \infty$ (blue), 4 (green), and 2 (red), as seen in the inset. In all profiles, the potential height was chosen as 3 eV, sufficient to confine the excited hole for all widths exceeding 3 nm. The remaining parameters are the same as those used in Figure 2.

DOI: 10.1021/nl903592h | *Nano Lett.* **2010,** *10,* 313-317

biexciton line in NC PL reported in ref 23 is direct evidence of Auger recombination suppression. Finally, García-Santamaría et al.[24] found that giant core/shell NCs, composed of relatively small cores surrounded by thick shells, have suppressed Auger rates. Although some of these results[24] were also connected with a softening of the confinement potential, more structural characterization is required for definite confirmation of this connection.

It is interesting to note the absence of Auger recombination in self-organized quantum dots with sizes comparable to those of typical NC quantum dots. In contrast to NC quantum dots, these self-assembled structures exhibit both trion and biexciton lines in their PL.[25] The difference could be connected with a much softer confinement potential created in the self-organization process by interdiffusion during the quantum dot overgrowth.

From Figure 2a, one can see deep minima having very narrow widths of just 1−2 Å. Could these rifts in the Auger recombination rate be observed experimentally? In ensemble measurements these minima will certainly average out due to a dispersion in NC sizes. Recently-achieved, precise control over NC size suggests that such magically sized NCs with suppressed Auger rates could be found. However, the efficiency of Auger process suppression will be diminished by random fluctuations of electric fields and temperature, which affect the effective height of the confinement potential. This may explain why "magically sized" NCs have not been observed before in single NC experiments, since their detection requires low temperature and low pumping intensity experiments.

In summary, we investigate how confinement potential size and shape affects the rate of nonradiative Auger processes. If the excited carrier has sufficient energy to enter the continuum, the Auger rate is proportional to the square of the Fourier amplitude of the initial ground state evaluated at the spatial frequency of the final excited state. Reducing the high spatial frequency components in the ground states by smoothing out the confinement can decrease the Auger rate by more than 3 orders of magnitude in comparison to a confinement with an abrupt boundary. Moreover, the calculations show that the Auger recombination rate undergoes strong oscillations as the confinement width is increased. In principle, this can allow fabrication of NCs having "magic sizes" that exhibit significant Auger recombination rate suppression. Such approaches can be utilized in engineering nonblinking NCs for use in biological and optoelectronic applications requiring high quantum efficiency. Finally, softening the confinement potential can also be used for engineering tunable, low-threshold lasers, and high quantum yield LEDs based on quantum wells and quantum wires of wide-gap semiconductors.

Acknowledgment. This work has been sponsored by the Office of Naval Research, the Alexander von Humboldt Foundation and the National Research Council Associateship Program.

Note Added after ASAP Publication. After this paper was published ASAP on December 17, 2009, additional changes were made; the corrected version was reposted on December 23, 2009.

Supporting Information Available. This material is available free of charge via the Internet at http://pubs.acs.org.

REFERENCES AND NOTES

(1) Shen, Y. C.; Mueller, G. O.; Watanabe, S.; Gardner, N. F.; Munkholm, A.; Krames, M. R. *Appl. Phys. Lett.* **2007**, *91*, 141101.
(2) (a) Fuchs, G.; Schiedel, C.; Hangleiter, A.; Härle, V.; Scholz, F. *Appl. Phys. Lett.* **1993**, *62*, 396. (b) Seki, S.; Oohasi, H.; Sugiura, H.; Hirono, T.; Yokoyama, K. *Appl. Phys. Lett.* **1995**, *67*, 1054.
(3) Chepic, D. I.; Efros, Al. L.; Ekimov, A. I.; Ivanov, M. G.; Kharchenko, V. A.; Kudriavtsev, I. A.; Yazeva, T. V. *J. Lumin.* **1990**, *47*, 113.
(4) Efros, Al. L.; Rosen, M.; Averboukh, B.; Kovalev, D.; Ben-Chorin, M.; Koch, F. *Phys. Rev. B* **1997**, *56*, 3875.
(5) Nirmal, M.; Dabbousi, B. O.; Bawendi, M. G.; Macklin, J. J.; Trautman, J. K.; Harris, T. D.; Brus, L. E. *Nature* **1996**, *383*, 802.
(6) Abakumov, V. N.; Perel, V. I.; Yassievich, I. N. *Nonradiative Recombination in Semiconductors*; North Holland: New York, 1991.
(7) Zegrya, G. G.; Kharchenko, V. A. *Sov. Phys. JETP* **1992**, *74*, 173.
(8) Kharchenko, V. A.; Rosen, M. *J. Lumin.* **1996**, *70*, 158.
(9) (a) Banin, U.; Bruchez, M.; Alivisatos, A. P.; Ha, T.; Weiss, S.; Chemla, D. S. *J. Chem. Phys.* **1999**, *110*, 1195. (b) Kuno, M.; Fromm, D. P.; Hamann, H. F.; Gallagher, A.; Nesbitt, D. J. *J. Chem. Phys.* **2000**, *112*, 3117. (c) Shimizu, K. T.; Neuhauser, R. G.; Leatherdale, C. A.; Empedocles, S. A.; Woo, W. K.; Bawendi, M. G. *Phys. Rev. B* **2001**, *63*, 205316. (d) Hohng, S.; Ha, T. *J. Am. Chem. Soc.* **2004**, *126*, 1324. (e) Fomenko, V.; Nesbitt, D. J. *Nano Lett.* **2008**, *8*, 287. (f) Chen, Y.; Vela, J.; Htoon, H.; Casson, J. L.; Werder, D. J.; Bussian, D. A.; Klimov, V. I.; Hollingsworth, J. A. *J. Am. Chem. Soc.* **2008**, *130*, 5026. (g) Protasenko, V.; Gordeyev, S.; Kuno, M. *J. Am. Chem. Soc.* **2007**, *129*, 13160.
(10) Efros, Al. L. *Nat. Mater.* **2008**, *7*, 612.
(11) Landau, L. D.; Lifshitz, E. M. *Quantum Mechanics*; Pergamon Press: Oxford, 1991.
(12) We remind the reader that an Auger transition will only occur if the final state decays much more rapidly than the Auger transition time. If not, the system will remain in a quantum superposition with an indeterminate final state.
(13) Efros, Al. L.; Efros, A. L. *Sov. Phys. Semicond.* **1982**, *16*, 772.
(14) Gossard, A. C. *J. Quantum Electron.* **1986**, *22*, 1649.
(15) Kane, E. O. *J. Phys. Chem. Solids* **1956**, *1*, 82.
(16) Further details can be found in the Supporting Information.
(17) Using boundaries larger than $L = 50$ nm smoothes out the small ripples seen in Fig. 2, but at the expense of increased processing time. Otherwise, larger boundaries have no significant impact on the results of our calculations.
(18) The Fourier transform of $1/(|x_1 - x_2| + \delta)$ has a logarithmic dependence as δ becomes small. When inserted into eq 8, this appears in the Auger rate as a weakly-changing, logarithmic factor that keeps the overall rate dependencies fixed.
(19) Rabani, E. Private communication.
(20) Wang, X.; Ren, X.; Kahen, K.; Hahn, M. A.; Rajeswaran, M.; Maccagnano-Zacher, S.; Silcox, J.; Cragg, G. E.; Efros, Al. L.; Krauss, T. D. *Nature* **2009**, *459*, 686.
(21) Klimov, V. I.; Mikhailovsky, A. A.; McBranch, D. W.; Leatherdale, C. A.; Bawendi, M. G. *Science* **2000**, *287*, 1011.
(22) Spinicelli, P.; Buil, S.; Quélin, X.; Mahler, B.; Dubertret, B.; Hermier, J.-P. *Phys. Rev. Lett.* **2009**, *102*, 136801.
(23) Osovsky, R.; Cheskis, D.; Kloper, V.; Sashchiuk, A.; Kroner, M.; Lifshitz, E. *Phys. Rev. Lett.* **2009**, *102*, 197401.
(24) García-Santamaría, F.; Chen, Y.; Vela, J.; Schaller, R. D.; Hollingsworth, J. A.; Klimov, V. I. *Nano Lett.* **2009**, *9*, 3482.
(25) Dekel, E.; Gershoni, D.; Ehrenfreund, E.; Spektor, D.; Garcia, J. M.; Petroff, P. M. *Phys. Rev. Lett.* **1998**, *80*, 4991.

DOI: 10.1021/nl903592h | *Nano Lett.* **2010,** *10,* 313-317